CHIN. PHYS. LETT. Vol. 38, No. 12 (2021) 126801

Li Plating on Carbon Electrode Surface Probed by Low-Field Dynamic Nuclear Polarization ^{7}Li NMR

Zhekai Zhang(张哲恺)[1,2], Jiyu Tian(田季宇)[3], Junfei Chen(陈俊飞)[1], Yugui He(贺玉贵)[1], Chaoyang Liu(刘朝阳)[1], Xinmiao Liang(梁欣苗)[1*], and Jiwen Feng(冯继文)[1]

[1]*State Key Laboratory of Magnetic Resonance and Atomic and Molecular Physics, Wuhan Center for Magnetic Resonance, Key Laboratory of Magnetic Resonance in Biological Systems, Wuhan Institute of Physics and Mathematics, Innovation Academy for Precision Measurement Science and Technology, Chinese Academy of Sciences, Wuhan 430071, China*

[2]*University of Chinese Academy of Sciences, Beijing 100049, China*

[3]*College of Chemistry and Molecular Sciences, Hubei Key Laboratory of Electrochemical Power Sources, Wuhan University, Wuhan 430072, China*

(Received 11 October 2021; accepted 16 November 2021; published online 25 November 2021)

Lithium deposition on graphite electrode not only reduces fast-charging capability of lithium ion batteries but also causes safety trouble. Here, a low-field ^{7}Li dynamic nuclear polarization (DNP) is used to probe Li plating on the surfaces of three types of carbon electrodes: hard carbon, soft carbon and graphite. Owing to the strong Fermi contact interaction between ^{7}Li and conduction electrons, the ^{7}Li nuclear-magnetic-resonance (NMR) signal of Li metal deposited on electrode surface could be selectively enhanced by DNP. It is suggested that low-field ^{7}Li DNP spectroscopy is a sensitive tool for investigating Li deposition on electrodes during charging/discharging processes.

DOI: 10.1088/0256-307X/38/12/126801

Lithium-ion batteries (LIBs) have been widely used in portable electronics because of their relatively high energy density and long cycle life. The extensive applications of LIBs in electric vehicle and stationary energy storage require higher energy and power density, longer lifetime and fast charging capability.[1,2] The performance of LIBs is strongly dependent on electrodes, electrolyte and their interfaces [often termed as solid electrolyte interphase (SEI)]. Among them, an SEI layer of high structure stability and high Li ion conductivity is crucial for high Coulombic and voltage efficiency,[3] long cycle lifetime[3,4] and safety[4,5] of the batteries. Generally, the composition and microstructure of an SEI layer are very complex, consisting of multiple organic and inorganic components appearing in either crystalline or amorphous form.[6] Understanding the atomic or molecular structure of each component in an SEI layer is still challenging.

A variety of techniques have been used to study the structure and distribution of chemical components in the SEI, including x-ray diffraction (XRD),[7,8] x-ray photoelectron spectroscopy (XPS),[9,10] Fourier transform infrared spectroscopy (FTIR),[11,12] electron paramagnetic resonance (EPR)[13,14] and nuclear magnetic resonance (NMR).[15,16] Solid-state NMR is a robust analytical method for providing atomic-level characterization on multiple chemical or structural components existing in SEI. However, NMR detection sensitivity is intrinsically low. This, together with the very low content of SEI phases in whole electrode material, makes it extremely difficult to acquire the NMR signal of concerned SEI phase. EPR has also been used in research of carbon materials. Matsumura *et al.* studied the lithium intercalation of banded carbon films with EPR and observed that the intercalation of Li can change the EPR strength and linewidth.[17] Subsequently, more and more researchers have studied the lithium intercalation characteristics of porous carbon, and discussed the changes of EPR spectra under the pore effect.[18,19] Recently, *in situ* EPR has been utilized to characterize Li deposition and intercalation of graphite anodes.[20] Usually, EPR signals from different kinds of unpaired electrons (or radicals) overlap due to small difference in g values, which make signal assignment very difficult. In addition, EPR can only be used to characterize the structure of molecules or ions bearing the unpaired electrons.

Fortunately, dynamic nuclear polarization (DNP) technology can generally improve the detection sensitivity of NMR signals by tens to hundreds of times.[21] DNP was first proposed by Overhauser in 1953.[22,23] It saturates EPR transitions to change the population of nuclear distribution through nuclear-electronic

Supported by the National Key Research and Development Program of China (Grant No. 2018YFC0115000), the National Natural Science Foundation of China (Grant No. 21603267), and the Chinese Academy of Sciences (Grant No. YZ201677 and YZ201551).

*Corresponding author. Email: xmliang@apm.ac.cn

© 2021 Chinese Physical Society and IOP Publishing Ltd

spin coupling, to greatly enhance the sensitivity of NMR. DNP can be used to characterize structures of both free radical and non-radical molecules (ions). In addition, it can also be used to directly study the state of intercalated lithium and its surrounding related electron, to establish the direct correlation between lithium and electrons in the lithium insertion site. DNP can also be used to investigate the Li metal deposition on carbon surface. Moreover, the unpaired free electrons of the deposited Li metal layers can also be utilized to enhance the NMR signal of the interface between the deposited Li metal and carbon matrix,[24] making it possible to selectively study the metal-carbon interface structure. Several recent DNP studies of battery materials illustrated that DNP-based NMR method is particularly useful in characterizing structures of both bulk electrode and SEI layer.[25,26] It is worth pointing out that all the reported DNP experiments so far on Li batteries were carried out on high-field DNP spectrometers (9.4 T or above) and at low temperature (∼100 K), which are very expensive. In general, the larger DNP enhancement could be more easily achieved at lower fields and with higher MW powers, without cryogenic sample cooling. Compared with the high-field DNP, the low-field DNP spectrometer accommodates larger sizes of samples, and is more easily constructed and equipped.[27,28] In addition, a low-field DNP spectrometer system has great potential in development of *in situ* SEI research.

In this Letter, we use DNP-enhanced ^{7}Li NMR spectra under a low magnetic field of 0.35 T to investigate the deposition of lithium metal on the surface of three types of carbonaceous electrodes materials including graphite, soft and hard carbons. For commercial LIBs, graphite (or carbon materials) is usually selected as the anode material due to its high lithium intercalation capacity and good reversible discharge-charge performances for lithium ions. It was reported that the deposition of lithium metal can occur on the surface of graphite anode upon fast charging, particularly at low temperatures.[29] The plating of lithium on a graphite anode hinders fast charging of lithium ion batteries, and results in fast degradation of electrode performance as well as causes the severe safety hazard.

Three types of carbon electrodes, e.g., graphite (GC, Shenzhen Saijiao Yang Energy Technology Co. Ltd, China), soft carbon (SC, BTR New Energy Material Co. Ltd, China) and hard carbon (HC, Kuraray Co. Ltd., Japan) were prepared by mixing 90 wt% GC/SC/HC and 10 wt% polyacrylic acid to form a slurry, which was then coated onto a copper (Cu) foil and dried at 60 ℃ overnight under vacuum. The area of the electrode was 1.13 cm^2, while the loading of the whole material was about 5 mg/cm^2. All the electrochemical measurements were conducted using 2032 coin cells with the above working electrodes, Li foil counter electrode, polypropylene microporous separator (Celgard 2400) and 1 M $LiPF_6$ in EC/DEC/PC (1:1:1 by volume) electrolyte. All the coin cells were assembled in argon-filled glove box with H_2O and O_2 content less than 1 ppm. The discharge tests were conducted on a Neware battery cycler at room temperature.

Electron paramagnetic resonance (EPR) spectra were recorded on a JEOL JES-FA200 spectrometer at room temperature. The samples (about 5 mg) were sealed in quartz tubes. The microwave power was 1 mW, and the modulation amplitude was 0.2 mT. Normal ^{7}Li NMR experiments were equipped on a home-made 500 MHz NMR spectrometer.[30] ^{7}Li DNP NMR spectra were obtained on our home-built 0.35 T DNP spectrometer with a typical DNP pulse sequence.[31] A long-time MW pulse operating at electron Larmor frequency (Overhauser DNP) was applied to excite the electron spin resonance so as to enhance the ^{7}Li NMR signal. The MW power and the pulse length for DNP are about 5 W and 0.5 s respectively. The ^{7}Li NMR chemical shifts were referenced to the LiCl (1 M) as 0 ppm.

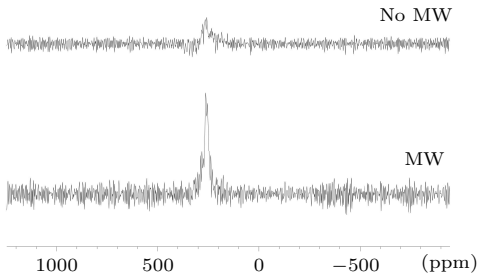

Fig. 1. ^{7}Li NMR spectra for Li metal powders with (lower) and without (upper) MW irradiation, using 8 scans and 12 scans, respectively, at 0.35 T.

Figure 1 shows the ^{7}Li NMR spectra of Li metal powders at room temperature under a magnetic field of 0.35 T with (lower) and without (upper) MW irradiations. ^{7}Li NMR signal appears around 260 ppm, which is due to the paramagnetic (Knight) shift caused by the Fermi contact interaction between ^{7}Li nuclei and conduction electrons. As can be seen in Fig. 1, the DNP-enhanced ^{7}Li NMR peak (lower) is significantly higher than the normal one (upper). By comparing the heights of two peaks, about six-fold positive DNP enhancement is yielded. In Li metal, ^{7}Li DNP enhancement is associated with rapidly fluctuating Fermi contact interaction between ^{7}Li and conduction electrons. Considering that lithium metal is a good conductor, the skin depths are ∼0.7 μm for MW irradiation at 9.5 GHz and ∼22.1 μm for rf irradiation at 8.7 MHz.[24] This means that EPR occurs in a much smaller sample region than NMR. After count-

ing in electron diffusion, the effective DNP depth is ∼10 μm, which is still significantly smaller than the rf skin depth (40 μm). Therefore, only part of the NMR region is DNP-active, leading to relatively small ^{7}Li DNP enhancement in Li metal powder.

EPR spectra for three types of carbon electrodes (hard carbon, soft carbon and graphite) in the normal Li-embedded state (∼170–200 mAh/g) and Li-overloaded (or over-discharged, ∼500 mAh/g) state are shown in Fig. 2. In the normal Li-embedded state, EPR signals of both hard and soft carbons are symmetric but with different peak-to-peak linewidths. EPR linewidth of the hard carbon (∼31 G) is obviously larger than that of the soft carbon (∼9 G), which can be ascribed to lower degree of graphitization or more disordered structure of the hard carbon. On the other hand, EPR spectrum of graphite in normal Li-embedded state exhibits an asymmetric dysonian lineshape typical for conduction electrons in the lithiated graphite (Li_xC_6, $x \leq 1$).[14] In the case of Li overloaded carbon electrodes, a very narrow signal with linewidth 0.06 G is overlapped with the abovementioned broad signal in all three types of carbon electrodes. Such a narrow EPR signal is assigned to the Li metal deposited on carbon electrodes, according to the reported EPR spectra of dendrite lithium with linewidth ∼0.05 G.[32]

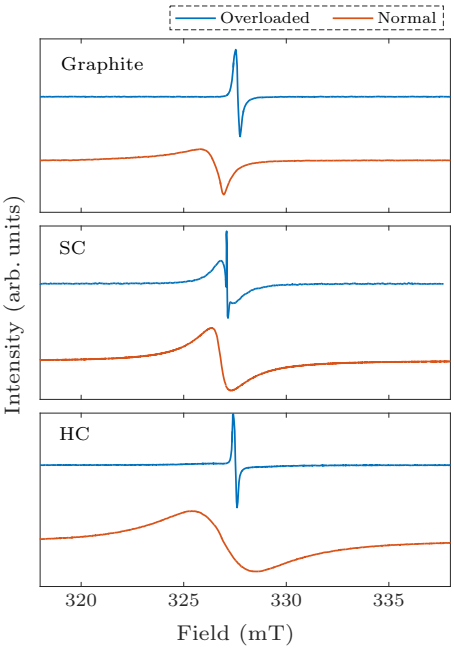

Fig. 2. EPR spectra from hard carbon, soft carbon and graphite electrodes in the normal Li-embedded state (lower) and Li-overloaded state (upper).

To further understand Li metal and Li-containing compounds in carbon electrodes, ^{7}Li NMR spectra at 11.7 T were acquired. Figure 3 shows the ^{7}Li NMR spectra for three types of carbon electrodes in the Li-overloaded state. A weak peak at ∼260 ppm can be seen in all the three samples and is ascribed to Li metal deposited on electrode surface. This indicates that Li metal deposition indeed occurs in the over-discharging process of LIB. The peak around 0 ppm is assigned to Li^+ ions from the residual electrolyte. The peaks at ∼20 ppm (HC) and ∼23 ppm (SC) are assigned to Li ions doped in hard and soft carbons, respectively. NMR signal for the intercalated Li in graphite appears at ∼50 ppm (LiC_6). Apparently, the chemical shift of ^{7}Li inserted in carbon matrix increases in order of hard carbon < hard carbon < graphite, which is consistent with the order of conductivity of three carbons. Higher conductivity (or conductive electron density) leads to a larger Knight shift. Compared the Li metal peak area with overall Li signal area, deposited Li metal fractions are estimated to be ∼20% for hard carbon and graphite electrodes and 4% for soft carbon electrode.

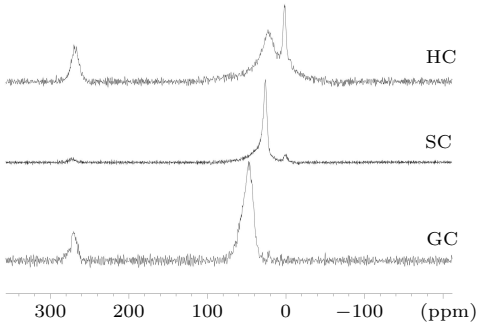

Fig. 3. ^{7}Li NMR spectra for three types of carbon electrodes in the Li-overloaded state with 1 scan at 11.7 T.

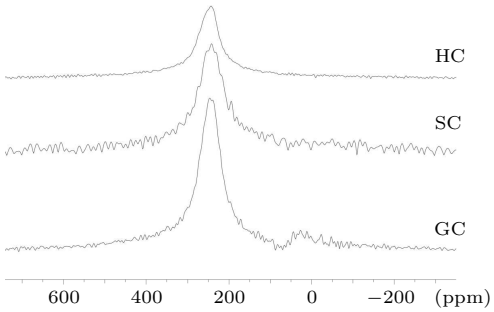

Fig. 4. DNP-enhanced ^{7}Li spectra for three Li-overloaded carbon electrodes with 256 scans.

Finally, DNP-enhanced ^{7}Li spectra for three Li-overloaded carbon electrodes were measured at static magnetic field of 0.35 T and the results are shown in Fig. 4. In Figs. 4(a) and 4(b), only single ^{7}Li NMR peak at ∼260 ppm from deposited metal is seen for both hard and soft carbons, while NMR peaks of intercalated ^{7}Li inside the hard and soft carbons are totally unobservable. For the graphite, on the other hand, besides abovementioned Li metal signal a weak ^{7}Li peak at ∼50 ppm from intercalated Li in graphite lattice is also observed. Note that all ^{7}Li peaks are not detected in the absence of DNP for all three electrodes even with 256 scans, due to extremely low detective

sensitivity of ^{7}Li NMR at a low field of 0.35 T. It can be roughly calculated via comparing ^{7}Li NMR intensities acquired with 0.35 and 11.7 T spectrometers, the signal strength at 11.7 T is about 200–350 times higher than that at 0.35 T. The error mainly comes from the very low signal-to-noise ratio of the measured signal at 0.35 T. The estimated metal ^{7}Li enhancements for SC, HC and graphite are about 40–70 times. The above results show that ^{7}Li signal from the deposited Li metal is significantly enhanced by DNP while ^{7}Li signal from the intercalated Li in graphite is also enhanced to some extent. For the deposited Li metal, the Fermi contact interaction between ^{7}Li and conduction electrons is very strong as evidenced by a large Knight shift of 260 ppm, which results in a large ^{7}Li DNP enhancement. Theoretically, the maximal ^{7}Li DNP enhancement in Li metal is about 1694. Because the normal ^{7}Li NMR signals are not observed in the carbon electrodes, we cannot directly determine the real ^{7}Li DNP enhancement from the deposited metal precisely. In this example, the DNP enhancement of the deposited lithium metal is estimated to be tens of times.

In general, ^{7}Li DNP enhancement in conductive materials is dominated by Overhauser effect associated with fluctuating scalar interaction or Fermi contact interaction between ^{7}Li and conduction electrons: upon irradiation of the conduction EPR transition, the cross relaxation between the electron and nuclei spins occurs simultaneously, thereby inducing nuclear polarization enhancement. In this case, the DNP enhancement factor ε can be expressed as[33]

$$\varepsilon \sim w_{0s} T_{1n} \left| \frac{\gamma_e}{\gamma_n} \right|, \tag{1}$$

where w_{0s} is the zero-quantum transition probability due to fluctuating Fermi contact interaction (moving free electrons); T_{1n} is ^{7}Li longitudinal relaxation time; γ_e and γ_n are respectively the gyromagnetic ratios of electron and nuclear spins; and s is the saturation factor of the electronic spin sub-system. As can be seen, DNP enhancement is directly proportional to w_{0s}, while w_{0s} is proportional to the conduction electron density at ^{7}Li nuclei. When lithium is intercalated into carbon layers, lithium is partially ionized. The Fermi contact interaction between ^{7}Li nuclei and the residual free electrons leads to Knight shift and Overhauser DNP enhancement of ^{7}Li NMR signal. For Li-intercalated graphite, the Fermi contact interaction between ^{7}Li and conduction electrons is relatively weak due to lower residual free electron density on Li nuclei, thus giving rise to a small DNP enhancement, compared with Li metal. Among three kinds of carbon materials graphite, soft and hard carbons, the conduction electron density of graphite is the highest, and thus the conduction electron density at ^{7}Li is expected also to be the highest, giving rise to the largest Knight shift and DNP enhancement. The above presented results demonstrate that DNP enhanced ^{7}Li spectrum even at a low magnetic field of 0.35 T could also be used to study very small masses of lithium metal deposited on electrode surfaces.

Both EPR and DNP can be used in the research of carbon materials. When the lithium ions intercalate between graphite (carbon) layers, both EPR intensity and linewidth change correspondingly, which reflects the characters of overall free electrons, and detailed structural information of the intercalated Li ion states cannot be yielded from the EPR experiment. Different from EPR, two important parameters in DNP NMR, i.e., Knight shift and DNP enhancement factor, are directly related to the residual free electron density on Li nuclei and thus can be used to characterize the state of intercalated lithium.

In summary, low-field ^{7}Li DNP at 0.35 T has been used to probe Li plating on three types of carbon electrodes, i.e., hard carbon, soft carbon and graphite, and the reported results are primary. Owing to the strong Fermi contact interaction between ^{7}Li and conduction electrons, the ^{7}Li NMR signal from deposited Li metal on electrode surface is selectively enhanced by DNP. ^{7}Li DNP NMR spectroscopy is found to be a sensitive tool to probe Li depositing on electrodes during charging/discharging processes. As we expect, *in situ* low-field DNP spectroscopy in combination with *in situ* EPR spectroscopy will be a promising approach for *in situ* investigation on Li metal deposition during rapid charge/discharge or aging of Li battery. In the future, we will use ^{7}Li DNP to investigate the kinetics of ^{7}Li deposition either inside holes or on the surfaces of different carbon materials under different conditions such as high charge/discharge rate and low temperature. A high-field DNP study on metal-carbon interface structure is under way, aiming at the mechanism of formation of Li metallic layer on carbon surfaces.

References

[1] Armand M and Tarascon J M 2008 *Nature* **451** 652
[2] Irisarri E, Ponrouch A and Palacin M R 2015 *J. Electrochem. Soc.* **162** A2476
[3] Sathiya M, Rousse G, Ramesha K, Laisa C, Vezin H, Sougrati M T, Doublet M L, Foix D, Gonbeau D and Walker W 2013 *Nat. Mater.* **12** 827
[4] Wen C J and Huggins R A 1981 *J. Electrochem. Soc.* **128** 1181
[5] Wen C J and Huggins R A 1981 *J. Solid State Chem.* **37** 271
[6] Gauthier M, Carney T J, Grimaud A, Giordano L, Pour N, Chang H H, Fenning D P, Lux S F, Paschos O, Bauer C, Maglia F, Lupart S, Lamp P and Shao-Horn Y 2015 *J. Phys. Chem. Lett.* **6** 4653
[7] Andersson A and Edström K 2001 *J. Electrochem. Soc.* **148** A1100
[8] Smart M, Ratnakumar B, Surampudi S, Wang Y, Zhang

X, Greenbaum S, Hightower A, Ahn C and Fultz B 1999 *J. Electrochem. Soc.* **146** 3963
[9] Andersson A M, Henningson A, Siegbahn H, Jansson U and Edström K 2003 *J. Power Sources* **119-121** 522
[10] Morigaki K I and Ohta A 1998 *J. Power Sources* **76** 159
[11] Ein-Eli Y, Markovsky B, Aurbach D, Carmeli Y, Yamin H and Luski S 1994 *Electrochim. Acta* **39** 2559
[12] Aurbach D, Levi M D, Levi E and Schechter A 1997 *J. Phys. Chem. B* **101** 2195
[13] Wandt J, Marino C, Gasteiger H A, Jakes P, Eichel R A and Granwehr J 2015 *Energy Environmental Science* **8** 1358
[14] Wandt J, Jakes P, Granwehr J, Eichel R A and Gasteiger H A 2018 *Mater. Today* **21** 231
[15] Gireaud L, Grugeon S, Laruelle S, Pilard S and Tarascon J M 2005 *J. Electrochem. Soc.* **152** A850
[16] Dai Y, Wang Y, Eshkenazi V, Peled E and Greenbaum S 1998 *J. Electrochem. Soc.* **145** 1179
[17] Matsumura Y, Wang S, Nakagawa Y and Yamaguchi C 1997 *Synth. Metals* **85** 1411
[18] Łoś, Duclauxb L, Kempiński W, and Połomska M 2010 *Microporous Mesoporous Mater.* **130** 21
[19] See K A, Hug S, Schwinghammer K, Lumley M A, Zheng Y, Nolt J M, Stucky G D, Wudl F, Lotsch B V and Seshadri R 2015 *Chem. Mater.* **27** 3821
[20] Wang B, Fevre L W L, Brookfield A, McInnes E J L and Dryfe R A W 2021 *Angew. Chem. Int. Ed.* **60** 21860
[21] Hooper R W, Klein B A and Michaelis V K 2020 *Chem. Mater.* **32** 4425
[22] Carver T R and Slichter C P 1953 *Phys. Rev.* **92** 212
[23] Overhauser A W 1953 *Phys. Rev.* **92** 411
[24] Hope M A, Rinkel B L D, Gunnarsdottir A B, Marker K, Menkin S, Paul S, Sergeyev I V and Grey C P 2020 *Nat. Commun.* **11** 2224
[25] Leskes M, Kim G, Liu T, Michan A L, Aussenac F, Dorffer P, Paul S and Grey C P 2017 *J. Phys. Chem. Lett.* **8** 1078
[26] Harchol A, Reuveni G, Ri V, Thomas B, Carmieli R, Herber R H, Kim C and Leskes M 2020 *J. Phys. Chem. C* **124** 7082
[27] Garcia S, Walton J H, Armstrong B, Han S and McCarthy M J 2010 *J. Magn. Reson.* **203** 138
[28] Rosay M, Tometich L, Pawsey S, Bader R, Schauwecker R, Blank M, Borchard P M, Cauffman S R, Felch K L, Weber R T, Temkin R J, Griffin R G and Maas W E 2010 *Phys. Chem. Chem. Phys.* **12** 5850
[29] Waldmann T, Hogg B I and Wohlfahrt-Mehrens M 2018 *J. Power Sources* **384** 107
[30] Yang L, Bao Q, Mao W and Liu C 2012 *Chin. J. Magn. Reson.* **29** 78 (in Chinese)
[31] He Y, Feng J, Zhang Z, Wang C, Wang D, Chen F, Liu M and Liu C 2015 *Rev. Sci. Instrum.* **86** 083101
[32] Niemoller A, Jakes P, Eichel R A and Granwehr J 2018 *Sci. Rep.* **8** 14331
[33] Liu G, Levien M, Karschin N, Parigi G, Luchinat C and Bennati M 2017 *Nat. Chem.* **9** 676